

Modeling the Radio Foreground for detection of CMB spectral distortions from Cosmic Dawn and Epoch of Reionization

Mayuri Sathyanarayana Rao^{1,2}, Ravi Subrahmanyam¹, N Udaya Shankar¹, Jens Chluba³

¹*Raman Research Institute, C V Raman Avenue, Sadashivanagar, Bangalore 560080, India*

²*Australian National University, Research School for Astronomy & Astrophysics, Mount Stromlo Observatory, Cotter Road, Weston, ACT 2611, Australia*

³*Jodrell Bank Centre for Astrophysics, University of Manchester, Oxford Road, M13 9PL, U.K.*

Email of corresponding author: mayuris@rri.res.in

ABSTRACT

Cosmic baryon evolution during Cosmic Dawn and Cosmological Reionization results in spectral distortions in the cosmic microwave background (CMB) owing to redshifted 21-cm absorption and emission. These spectral features from redshifts $30 \gtrsim z \gtrsim 6$ appear at meter wavelengths ($\lesssim 200$ MHz) as a tiny CMB distortion component in addition to the Galactic and extragalactic radio sky spectrum, which is orders of magnitude brighter. These spectral distortions encode information about the thermal history of baryons and the nature and timing of the first collapsed objects. However detecting them requires methods for precise modeling of foregrounds. Here we present an improvement over previous efforts to simulate foregrounds. We adopt GMOSS, a physically motivated sky model that represents sky spectra using radiative processes to simulate realistic expectation of sky spectra over 40–200 MHz. From mock observations resulting plausible spectral shapes we demonstrate that a polynomial of at least order seven is required to model foregrounds alone, indicating a greater level of spectral complexity in foregrounds than previously assumed. However, using polynomials to describe foregrounds results in a significant part of the EoR signal being potentially subsumed. As an alternative we demonstrate the benefits of adopting *Maximally Smooth* (MS) functions to model foregrounds. We find that foregrounds resulting from GMOSS are describable using MS functions and hence are smooth. Unlike polynomials, MS functions preserve EoR signal strength and turning points. We demonstrate that using a frequency-independent antenna and an ideal receiver of noise temperature 50 K, the global EoR signal can be detected with 90% confidence in ten minutes integration time, using MS functions to model foregrounds.

Subject headings: Astronomical instrumentation, methods and techniques - Methods: observational - Cosmic background radiation - Cosmology: observations - Reionization - Radio continuum: ISM

1. Introduction

The epoch of reionization (EoR) represents one of the important transitions in the physical state of the Universe, when the almost neutral baryonic matter from the Dark Ages transitioned to its mostly ionized form. Another important transition occurred earlier at even higher redshifts, when during the epoch of recombination the primordial plasma recombined and the Universe became neutral, with atomic

hydrogen, helium and a small fraction of light elements. While the physics of the epoch of recombination is well understood from the theoretical point of view (Chluba & Thomas 2011; Ali-Haïmoud & Hirata 2011; Glover et al. 2014) and constrained by observations of the Cosmic Microwave Background (CMB) (Planck Collaboration et al. 2016a; Calabrese et al. 2013; Farhang et al. 2013), EoR is relatively poorly understood. Among other aspects, the thermal evolution of baryons and nature of the first sources, the exact redshift and duration of reionization and the dominant mechanisms that affect reionization are poorly constrained (Planck Collaboration et al. 2016b). The evolution of the strength of redshifted 21-cm line of Hydrogen against the radiation from CMB is expected to trace the thermal history of the gas across EoR. Thus the redshifted 21-cm signal is predicted to appear as a distortion of the CMB spectrum, encoding the physics of EoR in the signal structure. A comprehensive review of EoR physics is presented in Furlanetto et al. (2006).

There are a multitude of scenarios that predict different global redshifted 21-cm signatures (see Pritchard & Loeb 2010). The form of the generic signature from EoR is shown in Fig. 1. The high redshift absorption feature ‘A’ at frequencies below about 30 MHz arises from collisional coupling of the spin temperature to the relatively low gas kinetic temperature. At relatively higher frequencies and below redshift of about 40 a second absorption dip ‘C’ arises from Wouthuysen-Field (Wouthuysen 1952; Field 1958) driving of spin to the kinetic temperature by Ly- α from the first collapsed objects. Subsequent X-ray and UV heating of the gas kinetic temperature, and consequently the spin temperature as well, by energetic radiation from the first stars and galaxies transforms the appearance of the gas from absorption to emission (at ‘D’); the ionizing radiation then progressively results in the disappearance of the baryons in redshifted 21 cm and the gas is fully ionized and vanishes from this diagnostic by redshift 6 (at ‘E’). The critical spectral features representing events in the thermal history, which appear as turning points and successive absorption and emission features, are in the frequency range 10–200 MHz corresponding to events at redshifts of about 150 to 6. Detection of the reionization signature is a way to constrain the parameter space of the sources of reionization and their spatial-temporal distribution.

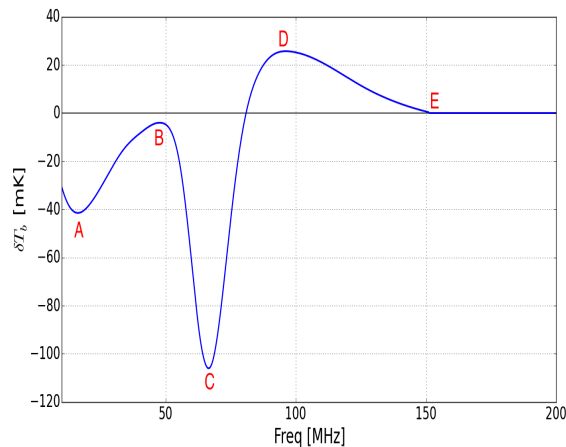


Fig. 1.— The generic redshifted 21-cm EoR signature expected in the frequency range 10 to 200 MHz from thermal evolution in baryons at redshifts 150 to 6. This is expected to appear as a global spectral distortion in the spectrum of the cosmic microwave background.

At meter and decameter wavelengths, where the global EoR signal resides, foregrounds due to Galactic and extragalactic radio sources are relatively bright. The reionization signals are of 10–100 mK brightness temperature whereas the foregrounds are 100’s to 10,000’s of K; the spectral dynamic range required for the detection of the global EoR signature in any measurement of the absolute spectrum of the radio sky is about 10^3 – 10^6 . It is therefore not surprising that considerable effort has been on development of methods for separation of the faint 21-cm signals from the substantially brighter foreground component in measurement data (Gnedin & Shaver 2004; Harker 2015).

2. Motivation

Several ongoing and proposed experiments to detect the global EoR signal exist. Nevertheless, the methodology for the modeling, subtraction of foregrounds and extraction of the much smaller EoR signal from spectral data, or for joint modeling of foregrounds and EoR signals, continues to be an open problem.

The EDGES experiment (Bowman & Rogers 2010) observed the sky spectrum in the frequency range 100 to 200 MHz and excluded rapid reionization with timescales less than that corresponding to $\Delta z < 0.06$. Polynomials of different orders in different frequency windows were used to jointly fit and model the foreground and instrumental systematics. The BIGHORNS experiment (Sokolowski et al. 2015) used a ninth-order polynomial to model the receiver noise, and the Global Sky Model (GSM) of de Oliveira-Costa et al. (2008), together with the simulated radiation pattern of their antenna, to estimate the foreground contribution in their data. The SCI-HI 21-cm all-sky experiment (Voytek et al. 2014) also used the interpolated GSM to calibrate the foreground in their data. These approaches come with several problems. First, modelling with polynomials of arbitrary order inclusive of GSM based models, which also employ mathematical interpolation between measurements from publicly available all-sky radio surveys, can be unrealistic in their spectral shapes. Second, estimates of the percentage loss in EoR signal on subtracting a polynomial baseline, and the level of foreground contamination that may remain in the residual, suggest that such a simple polynomial or GSM approach to modeling the foreground component in spectral data is far from ideal (Pritchard & Loeb 2010; Voytek et al. 2014; Harker 2015).

A spectral radiometer connected to an elemental antenna provides as its response a measurement set that contains the signature arising from baryon thermal evolution and reionization of Hydrogen gas along with the orders of magnitude larger foreground component. This radio foreground component appears as an average of sky spectra over the beam pattern of the telescope antenna. Even though the foreground might be composed of emitting volume elements that individually have spectra of power-law form, the variation in the spectral indices of these sources along the line of sight and across the sky within the antenna beam results in an observed spectrum in which the foreground component has an unknown form and cannot be modeled as a simple power law anymore.

The order of the polynomial deemed necessary to fit foreground components in spectral data to \sim mK level, lower than the expected signal, has varied in literature depending on the assumed sky model. Pritchard & Loeb (2010) argue that averaging sky spectra over large angular scales by wide-angle beams of telescopes designed for the global EoR detection would result in smooth frequency dependence for the foregrounds in spectral data and a third-order polynomial may suffice to model the foreground component and reduce their residuals to well below the expected EoR amplitude. But they point out that these residuals are dominated by the numerical limitations of available sky models and also recognize that a simple polynomial approach to modeling the foreground—with order sufficient to describe the foreground and systematics in spectral

data—could substantially diminish the desired EoR signal in the residual. More recent results suggest the need to adopt polynomials of higher order (> 4) to model foregrounds to mK levels in measurements to be able to discern the global EoR signal (see Bernardi et al. 2015). However, while polynomials of lower order might not model the foreground components with sufficient precision, polynomials of higher orders risk over fitting the foregrounds and partially removing the EoR signal of interest in the process. Adoption of sky models with increasing complexity while generating synthetic spectra and mock observations in general leads to concluding that a higher order in the polynomial is required to fit to the foreground components in the mock observations so as to be able to discern the EoR signal. This uncertainty in inferences of the degree of the polynomial required to model the foreground in measurements with sufficient precision arises both due to differences in the assumed spectral structure in the sky brightness and due to instrumental effects. In the light of uncertainty in both the global EoR signal as well as in models for the low frequency sky ($\lesssim 200$ MHz), appropriate choice of the functional form adopted to model the foreground in spectral data is critical to interpreting any global EoR signal detection experiment, failing which results in unknown biases in interpretation of data.

In the present work, we examine mock sky spectra as recorded by an antenna with a wide field of view and a frequency-independent beam. We compare the order of polynomials required when fitting to mock spectra generated with different assumed sky models. However, we do not examine instrumental effects on detecting the global EoR signal, such as the mode coupling of spatial structures in the sky to the measured spectrum in frequency (see Mozdzen et al. 2016).

This paper represents an improvement on previous work in two ways. First, we use a new physical sky model, GMOSS (Sathyanarayana Rao et al. 2016), that models the radio spectrum over the sky using parameters that describe radiative processes, which are fit to a set of all-sky maps. This is an improvement over polynomial or other interpolations between measured sky brightness at discrete and widely spaced frequencies in that the present approach results in synthetic spectra that have physical and plausible spectral forms. Second, we use a new functional form for describing the foreground component in measurements, namely *maximally smooth* functions. This functional form for the foreground was recently applied to simulations of the detection of primordial recombination-line ripples from redshift $z \simeq 1000$ (Sathyanarayana Rao et al. 2015), where it was demonstrated that this approach is indeed powerful. We examine detection likelihoods when mock observations are jointly modeled using theoretical EoR templates and *maximally smooth* functions to describe the foreground. We demonstrate that for the more realistic physical GMOSS model of the foreground, the proposed modeling of foregrounds in measurement sets using *maximally smooth* functions is robust and superior to the more simplistic polynomial-form representation.

3. Towards a spectral model for the radio sky

Previous efforts to simulate data analysis methods for global EoR signal detection experiments have assumed simple sky models that are, in log-temperature vs log-frequency space (hereinafter referred to as $\log(T)$ vs $\log(\nu)$ space), either power laws or low-order polynomials (see, for example, Pritchard & Loeb 2010; Harker 2015). The method adopted to separate the signal from foregrounds in mock observations is to fit the simulated spectra with polynomials of low order, possibly identical to those used to generate the input model sky. Clearly, since the EoR signal contains higher-order inflections than those used to describe the sky spectrum and model the foreground in data, this would leave behind in the residual a substantial part of the EoR signal. Such a simplistic input model for the sky with subsequent modeling of the foreground components in mock observations using polynomials of matching order belies the challenge when dealing

with real measurements where the true functional form of the sky spectrum and that of the foreground component in data are unknown.

In this section, we generate synthetic sky spectra without any EoR component by using different plausible sky models and estimate the degree of polynomial required to model the foreground in mock data to mK precision in each case. Spectra with greater spectral complexity, in $\log(T)$ vs $\log(\nu)$ space, require a polynomial of higher degree to fit to the desired level. Combining spectra from individual pixels can result in a final beam-weighted mock spectrum of different spectral complexity. We investigate the consequences of adopting three separate sky models on the deduced order of the polynomial required to fit the final beam-weighted foregrounds to mK level. Pixel spectra are described in these three cases as (i) power laws or linear functions in $\log(T)$ vs $\log(\nu)$ space, (ii) polynomials in $\log(T)$ vs $\log(\nu)$ space and (iii) the Global MModel for the radio Sky Spectrum (GMOSS; Sathyanarayana Rao et al. 2016).

In each of these models, spectra are derived via spectral fits that are done separately at each sky pixel that is 5° in size. The spectral fits are then averaged over wider beams to generate the final mock spectrum as might be observed with a telescope that has a wide field of view. The fits are made to a set of six measurements at discrete frequencies, which are from a set of six all-sky maps. The maps used are at 150 MHz (Landecker & Wielebinski 1970), 408 MHz (Haslam et al. 1982), 1420 MHz (Reich 1982; Reich & Reich 1986; Górski et al. 2005) and 23 GHz (WMAP science data product¹). The treatment of various maps to bring them to their final usable form are presented in Sathyanarayana Rao et al. (2016). Maps at 22 and 45 MHz are generated from the Global Sky Model (see de Oliveira-Costa et al. 2008). In their final form, all input maps have a common resolution of 5° and are represented in galactic coordinates in nested ‘R4’ scheme of HEALPix. Our code uses these sky images to generate synthetic sky spectra at any location on Earth and at any local time, including appropriate corrections for effects including precession and atmospheric refraction. Unless otherwise specified, we assume observing with an antenna having a frequency independent beam with half power beam width (HPBW) of 78° . In the three subsections below, the antenna is assumed to be pointed towards zenith and observes the sky over Gauribidanur Observatory in southern India, which is at latitude $13^\circ 01$ N and longitude $77^\circ 58$ E. The mock data are assumed to be recorded by a correlation spectrometer with in-built calibration for instrument bandpass with 1 MHz frequency resolution. We focus on the frequency range 40–200 MHz where the EoR signal is predicted to be present.

3.1. Case of power-law form for sky spectra

Galactic synchrotron emission, which dominates the low-frequency radio sky (in our context $\nu \lesssim 1$ GHz), may in its simplest form be described as a power law:

$$T(\nu, n) = T_{\nu_0, n} \times \left(\frac{\nu}{\nu_0}\right)^{\alpha(n)}, \quad (1)$$

which in $\log(T)$ vs $\log(\nu)$ space has a linear form:

$$\log(T(\nu, n)) = \log(T_{\nu_0, n}) + \alpha(n) \times \log\left(\frac{\nu}{\nu_0}\right). \quad (2)$$

Here $T(\nu, n)$ is the brightness temperature at frequency ν towards pixel n and $\alpha(n)$ is the temperature spectral index of the power-law emission in that sky pixel. $T_{\nu_0, n}$ is the temperature at frequency $\nu = \nu_0$ towards pixel n .

¹WMAP Science Team.

We realize an all-sky model by computing at each sky pixel such a power-law spectrum by a straight-line fit to the data points given by the six maps towards that pixel. Fits done in $\log(T)$ vs $\log(\nu)$ space, as given by Equation (2), weight the data to have uniform fractional errors. Mock spectra, without any EoR signal added, were generated at times spaced 1 hr apart over the full LST range 0–24 hr by averaging the pixel spectra with a weighting defined by the telescope beam at each time. The sample mock spectra are representative of the complexity in inherent spectral structure that might be expected for the foreground component. We show in Fig. (2) the form of the residuals on fitting with polynomials of a few orders for representative spectra, which correspond to LSTs when the beam is on and off the Galactic plane. The amplitudes of residuals on fitting these spectra with a polynomial of order two are a few mK, with residuals somewhat larger for mock observations towards the Galactic plane.

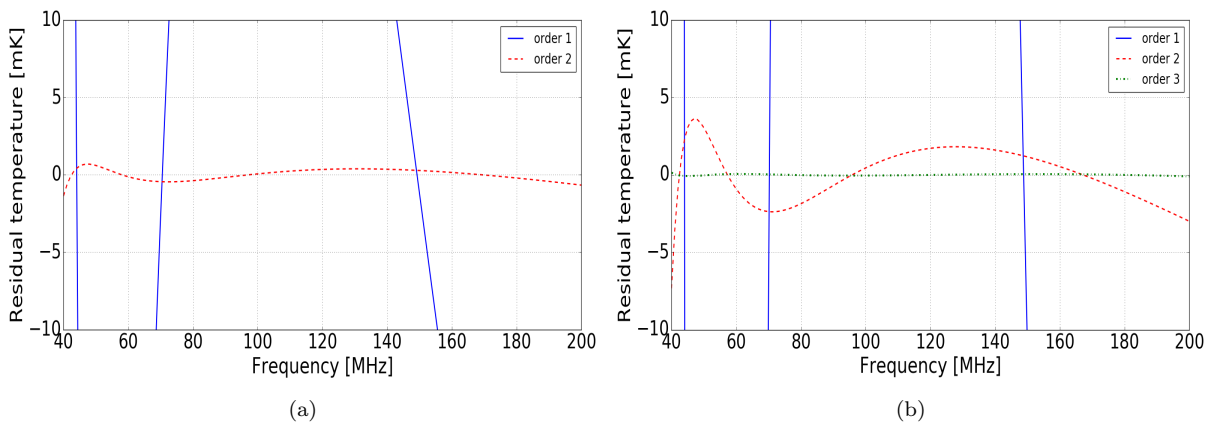


Fig. 2.— The residuals obtained on fitting to mock observations of the foreground sky in $\log(T)$ - $\log(\nu)$ space with polynomials of first order (blue solid line) and second order (red dashed line). The sky spectra were generated from a model sky that assumes a simple power-law form radio spectrum at each sky pixel. The panel on the left are residuals obtained for a mock observation that is away from the Galactic plane and the one on the right corresponds to a mock spectrum that includes the Galactic plane.

If we assume a power-law spectral form for sky spectra at every pixel that lies in a telescope beam, we conclude that the beam-averaged foreground spectra might be fit with a quadratic polynomial with an accuracy that allows discerning the generic EoR signal.

3.2. Case of a polynomial sky model

The six data points in the input sky-maps do not lie on a straight line at every pixel in $\log(T)$ vs $\log(\nu)$ space. Clearly, the emission from the foreground, even in single pixels, is not precisely describable as a single power law. We allow for curvature in the sky spectrum in $\log(T)$ vs $\log(\nu)$ space by fitting the six data points at each pixel with a fifth order polynomial:

$$\begin{aligned} \log(T(\nu, n)) = \log(T_{\nu_0, n}) + \alpha(n) \times \log\left(\frac{\nu}{\nu_0}\right) + \beta_2(n) \times \log\left(\frac{\nu}{\nu_0}\right)^2 + \beta_3(n) \times \log\left(\frac{\nu}{\nu_0}\right)^3 \\ + \beta_4(n) \times \log\left(\frac{\nu}{\nu_0}\right)^4 + \beta_5(n) \times \log\left(\frac{\nu}{\nu_0}\right)^5, \end{aligned} \quad (3)$$

where the $\beta_i(n)$ coefficients provide for higher order curvature in the spectrum.

The optimized best-fit coefficients to such a quintic form at every pixel provides an input sky model to the pipeline described above. As above, we generate beam-convolved sky spectra for different LSTs over 0–24 hr and fit these with polynomials of varying order. The residuals so obtained for two such realizations of the sky for LSTs corresponding to off and on the Galactic plane are in the left and right panels of Fig. (3) respectively. Clearly, if we adopt a quintic polynomial model for sky spectra, and seek to model the foreground components in measurements to an accuracy so as to limit residuals to mK levels, polynomials of order four are required off the Galactic plane and orders about 5–6 are required for telescope pointings towards the Galactic plane.

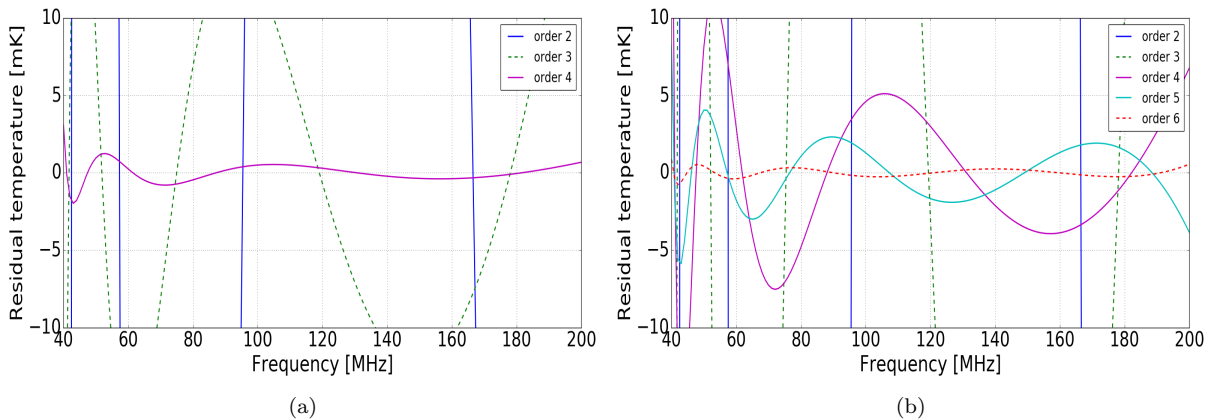


Fig. 3.— Residuals on fitting mock spectra, generated from a model that assumes a quintic form for the spectrum at each pixel, with polynomials of increasing orders. The panel on the left are residuals obtained for a mock observation that is away from the Galactic plane and the one on the right is for a mock spectrum that is towards the Galactic plane.

The above exercise demonstrates that if a higher level of complexity is allowed for the spectral structure in the model for the foreground, a higher order of polynomial is necessary to fit the mock observations that simulate beam-averaged spectra. The spectral structure inherent in the sky model in simulations thus critically guides strategies developed to deal with foregrounds in measurements. Increasing the order of the interpolating polynomial to create sky models that are cubic, quartic, quintic, and so on require increasingly greater orders of polynomials for modeling the foreground component in mock observations. Additionally, using higher-order polynomials to model foregrounds risks generating unphysical sky models that would no longer usefully guide detection strategies.

Since there are a limited number of maps (data points) available, and the uncertainties in individual maps are orders of magnitude greater than the precision required for detection of EoR, and with no physical rationale to guide the order of the interpolating polynomial, we shift gears towards a physically motivated sky model as described below.

3.3. GMOSS: Global Model for the radio Sky Spectrum

GMOSS (Sathyanarayana Rao et al. 2016) is a physically motivated model of the radio sky spectrum, in which seven physical parameters define the radiative processes that generate the spectrum of the brightness at each sky pixel. GMOSS incorporates plausible physics including (i) synchrotron emission that is assumed

to arise from a power-law form electron energy spectrum that may have a break as well, (ii) composite emission from flat and steep spectrum synchrotron sources, (iii) thermal absorption at low frequencies and (iv) optically thin thermal free-free emission at high frequencies. GMOSS provides synthetic spectra representative of the intensity distribution towards HEALPix pixels of 5° over the whole sky, and these are averaged over telescope beams to yield mock observations.

Residuals on fitting polynomials of varying order to such mock observations are given in Fig. (4a) and Fig. (4b) for two LSTs where the telescope beam points off and on the Galactic plane respectively. The complexity in spectral structure due to the underlying physical processes necessitates a polynomial of order seven in $\log(T)$ vs $\log(\nu)$ space to fit the mock observations of the foreground to an accuracy sufficient to be able to limit residuals to a few mK and hence discern the EoR signal.

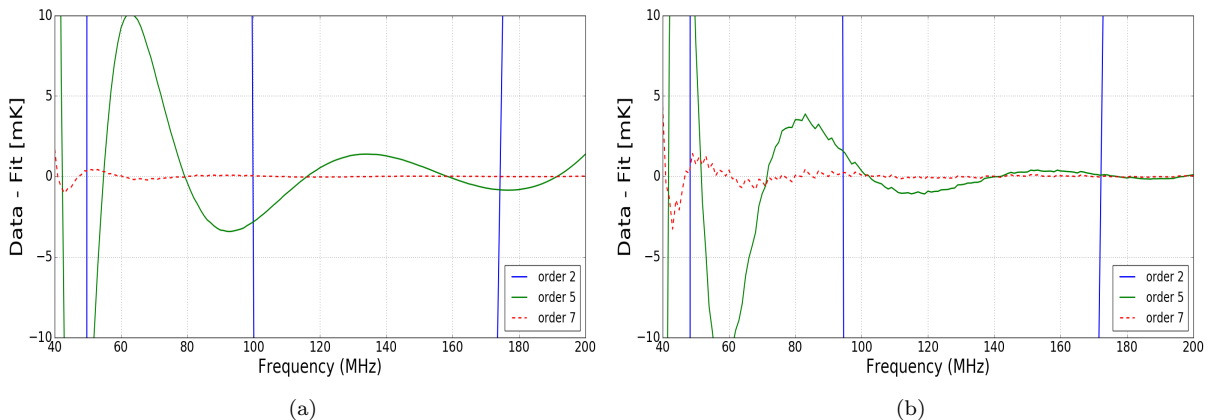


Fig. 4.— Residuals on fitting mock spectra, generated from a model that assumes GMOSS as the sky model, with polynomials of increasing orders. The panel on the left are residuals obtained for a mock observation that is away from the Galactic plane and the one on the right is for a mock spectrum that is towards the Galactic plane.

We infer that increasing the complexity of the model that describes the foreground demands, unsurprisingly, higher-order polynomials to model the mock observations to sufficient accuracy for detection of EoR. This trend is shown in Fig. (5), which plots the root mean square (RMS) of residuals against the polynomial order; these residuals were obtained on fitting mock observations generated assuming the three different sky models. When the order of the fitting polynomial is increased to a sufficiently large value, all curves will eventually reach an asymptotic RMS level corresponding to the numerical noise inherent in the mock spectra. The solid lines represent residuals corresponding to spectra away from the Galactic plane and the dashed lines are for those looking at the Galactic plane.

Although at first glance a low RMS residual might be encouraging, it may be noted that increasing the order of the fitting polynomial would also fit to the EoR signal thus subsuming the EoR signal into the estimate of the foreground and hence compromising the detection. This is demonstrated by fitting polynomials of varying order to mock observations that also contain the generic vanilla model for the EoR signal. GMOSS is adopted for describing the foreground sky spectrum since it is physically motivated and most realistic. The residuals in this case are shown in Fig. (6). Increasing the order of the polynomial changes the form of the residual: the peak amplitude of the residual progressively diminishes and the number of turning points in the residual increases, and thus the residual progressively departs from the form of the

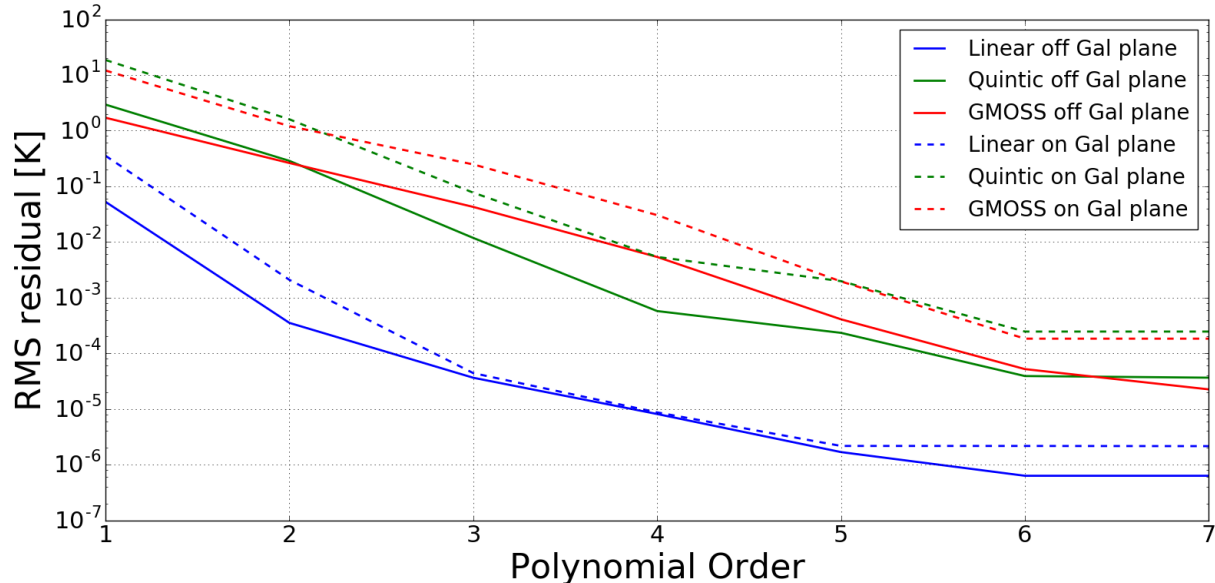


Fig. 5.— RMS of residuals on fitting mock observations of foregrounds, which are generated using different sky models, versus the order of the fitting polynomial. Solid lines are for mock observations that are recorded away from the Galactic plane and the dashed lines are for those that are towards the Galactic plane.

generic vanilla model for the EoR signal.

To fit and subtract foregrounds, or for joint modeling of the foreground with the EoR signal, without compromising the information contained in the EoR signal and preserving the turning points and amplitude of the signal, we propose below that foreground components of spectral radiometer measurements be modeled not with polynomials but with Maximally Smooth (MS) functions.

4. Modeling the foreground using Maximally Smooth functions

Due to its physically motivated nature that leads to mock sky spectra with plausible complexity, we hereinafter adopt GMOSS as the sky model. As has been demonstrated in Sathyanarayana Rao et al. (2016), individual pixels (5° wide) may have spectral shapes that can be described as being concave, convex or of more complex shape. We now examine whether beam-averaged mock spectra generated using GMOSS are smooth in the sense that they do not have embedded small-amplitude ripples that may confuse a detection of fine-scale cosmological signals from reionization.

We use Maximally Smooth (MS) functions (see Sathyanarayana Rao et al. 2015) as a generic form to describe smooth spectra. An MS function $f(x)$ is a polynomial of degree n

$$f(x) = p_0 + p_1(x - x_0) + p_2(x - x_0)^2 + p_3(x - x_0)^3 + p_4(x - x_0)^4 + \dots + p_n(x - x_0)^n \quad (4)$$

in which the polynomial coefficients p_j are constrained so that there are no zero crossings within the domain

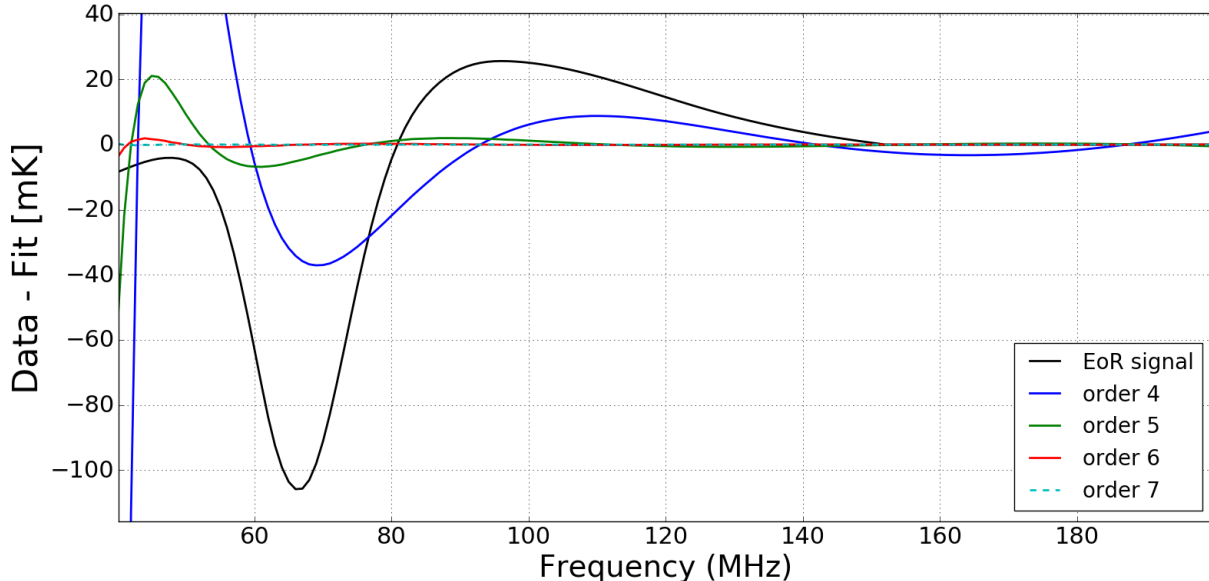


Fig. 6.— The residuals obtained on fitting a mock observation of the sky spectrum, which uses GMOSS as the sky model and also contains the EoR signal, with polynomials of orders 4, 5, 6 and 7. Overlaid as a solid black line is the generic prediction for the EoR signal. Increasing the order of the polynomial used, in $\log(T)$ vs $\log(\nu)$ space, to model and remove the foreground component of the spectrum results in a residual that progressively departs from the form of the generic EoR signal. Not only does the amplitude of the EoR signal reduce, additional turning points in the signal are also introduced.

for any derivative of order $m \geq 2$. The order- m derivative of the polynomial is

$$\frac{d^m f(x)}{dx^m} = \sum_{i=0}^{n-m} \{(m+i)!/i!\} p_{m+i} (x-x_0)^i \quad (5)$$

and the coefficients p_j are constrained so that for all m in the range 2, 4, ..., $(n-1)$ the above derivative functions are never zero within the domain of interest. Critical to the modeling is the formulation of a robust method for solving for the parameters: the coefficients of the MS polynomial are solved for by successively approximating the function as a Taylor expansion about a point x_0 within the domain, which is also a free parameter. The order of the MS function is increased by one in each iteration and the parameters returned in the previous step are used as initial guess in the next.

Constraining the polynomial in this manner while fitting to the measured sky spectrum in $\log(T)$ - $\log(\nu)$ space allows the function to fit to the mean spectral index, a constant spectral curvature and higher order curvatures without allowing the polynomial to follow any ripple or multiple turning points in embedded spectral components.

As a first step, we examine the residuals on fitting the adopted generic form of the EoR signal with MS functions and compare with residuals on fitting with polynomials that have no constraints on coefficients. We present in Fig. (7) residuals on fitting the global EoR signal, which has multiple turning points over the 40–200 MHz band and is hence not Maximally Smooth, with polynomial and MS functions of varying orders. We add the CMB monopole temperature to the global EoR signal and then fit the resulting spectrum in

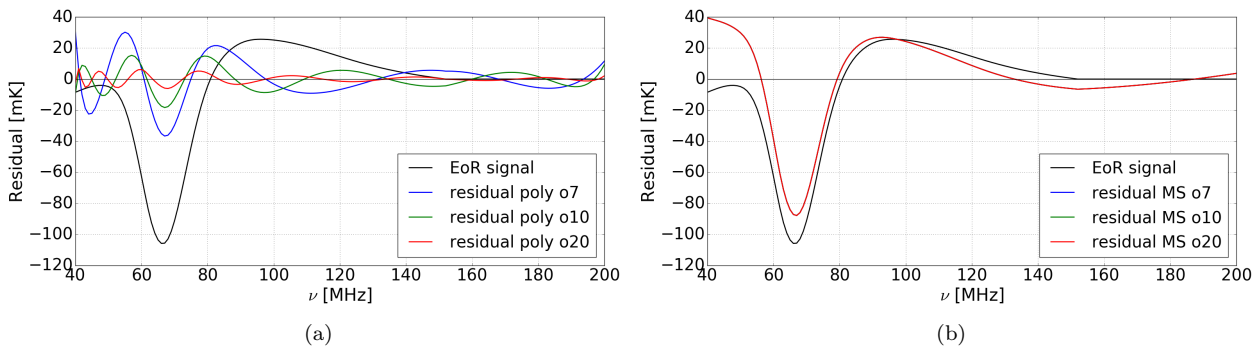


Fig. 7.— Residuals on fitting the global EoR signal with varying orders of (a) polynomials and (b) MS functions; fits are made in $\log(T)$ - $\log(\nu)$ space to the assumed global EoR signal plus a CMB with temperature $T_0 = 2.73$ K. Residuals to polynomial fits substantially differ from the EoR signal assumed, displaying reduced amplitude as well as multiple turning points. On the other hand, fitting the EoR signal with an MS function of arbitrary order preserves turning points and after the smooth component of the signal is entirely removed, the residual saturates and does not change any further on increasing the order of the MS function as evidenced by the curves of all residuals lying perfectly one above the other. Shown as a black solid line in both panels is the global EoR signal that is being fit to. A polynomial of order at least 7 is adopted as is necessitated by GMOSS, as described in Section 3.3.

$\log(T)$ - $\log(\nu)$ space. Since foregrounds generated using GMOSS as the sky model require at least a 7th order polynomial in $\log(T)$ - $\log(\nu)$ space to fit to the accuracy needed for global EoR detection, we fit foregrounds with polynomials of orders 7, 10 and 20. As shown in Panel (a) of Fig. (7), modeling the EoR signal with polynomials results in turning points being introduced in the residual, which were not present in the EoR signal itself. As a consequence, the shape of the residual is no longer qualitatively similar to the cosmological signal. Further, the amplitude of the residual progressively reduces and if fit with a sufficiently high-order polynomial the signal risks being entirely fitted out and hence subsumed in any polynomial model for the foreground. As a comparison, residuals on modeling the same spectrum with MS functions of orders 7, 10 and 20 are shown in Panel (b) of Fig. (7). Clearly, the residual obtained on fitting MS functions retains all the turning points of the EoR signal. The residual is not identical to the EoR signal itself and represents a smooth baseline subtracted version of the signal. Additionally, increasing the order of the MS function does not deteriorate the amplitude of the signal in the residual once all the smooth components in the data have been removed. This suggests that if the only non-smooth component in a measurement is the EoR signal itself, fitting an MS function of arbitrarily high order should leave behind in the residual a distinctive signature of the EoR signal with all turning points intact and with minimal degradation of signal strength.

As a second step, we examine whether beam-averaged mock sky spectra generated using GMOSS as the sky model are indeed maximally smooth, at least to the precision needed to detect an embedded generic EoR signal. We generate mock sky spectra at different observing sites to include different parts of the sky, and hence investigate smoothness of spectra over different samplings of sky coverage and spectral complexity. At any observing site, we generate 24 mock sky spectra one hour apart and with a uniform sampling over LST. The observing sites adopted for the simulations were (a) Hanle in North India where the Indian Astronomical Observatory is situated (Latitude = 32.79°N) and (b) Murchison Radio Observatory (MRO) site in Western Australia (Latitude = 26.68°S). With large antenna beams as are typically employed by most global EoR detection experiments (see Raghunathan et al. 2013), it is impossible to completely avoid the Galactic plane

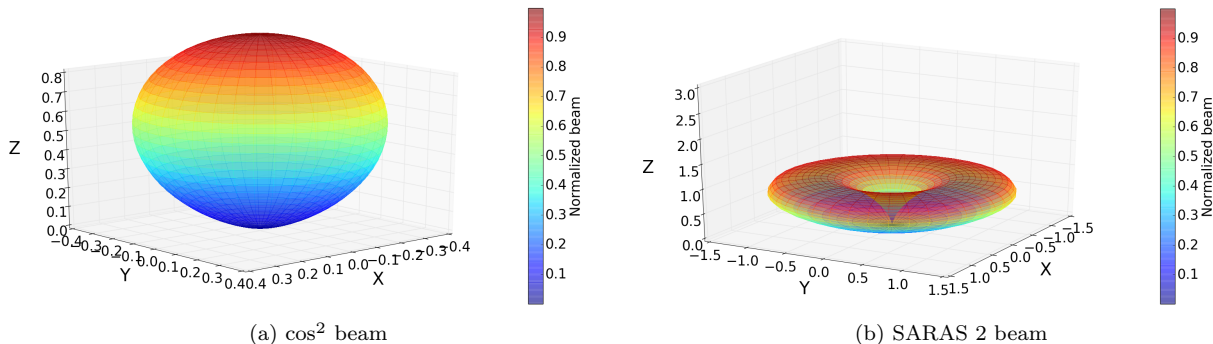


Fig. 8.— Frequency-independent antenna beam patterns adopted in simulations of mock sky spectra. The \cos^2 beam pattern in panel (a) represents a beam with a peak towards the zenith. The SARAS 2 beam in panel (b) on the other hand has a null towards the zenith and a peak towards an elevation of 30° . Both beams have a null towards the horizon. The beam shapes have been chosen to be complementary to one another and provide different beam weighted samplings of the sky.

from any observing site on Earth. Mock sky spectra were generated by simulating observations with (a) an ideal frequency-independent \cos^2 beam pattern that has maximum towards zenith (see Figure 8a) and (b) adopting the short-monopole type beam pattern of the SARAS 2 ² antenna that has null towards zenith, null towards horizon and maximum towards elevation of about 30° (see Figure 8b). The choice of observing sites, close to $+30$ and -30 degrees of latitude, and beams that are contrasting in shapes, was made to have a wide variety in plausible spectra. The final calibrated mock spectra in each case are generated over the 40–200 MHz band and have, in addition to the foreground spectrum, contribution from the CMB.

Though in the frequency range of interest (40–200 MHz) the difference between the Planck form and its Rayleigh-Jeans approximation is about 1 Jy sr^{-1} in specific intensity, we still explicitly fit to the CMB using its Planckian form to avoid any spectral shapes that may arise from approximately modeling the CMB as a constant in brightness temperature.

Thus the functional form used to describe the mock spectrum is

$$T(\nu) = \left(\frac{h\nu}{k}\right) / \left(e^{\frac{h\nu}{kp_0}} - 1\right) + 10^{\sum_{i=0}^N [\log_{10}(\nu/p_1)]^i p_{i+2}}. \quad (6)$$

Here p_0 is the CMB temperature, p_1 is the point about which the Taylor expansion is centered and p_2 through p_{2+n} are the coefficients of the terms in the N^{th} -order Maximally Smooth function that models the foreground. The remaining terms follow the standard notation.

The mock spectra representing the foreground and undistorted CMB at different LSTs and for different sites and telescope beams were all uniformly fit with Maximally Smooth functions of order 10. Sample spectra corresponding to LSTs when the antenna temperatures are minimum and maximum, the corresponding sky coverage by the telescope beam for each of these spectra, and the residuals on fitting these spectra with the function given by above Equation 6, are shown in Fig. (9). The sky-coverage plots give the all-sky map at 150 MHz with a resolution of 5° such that pixels that lie outside the beam are blanked. To examine for just the smoothness of foregrounds, these mock spectra have not had the EoR signal added.

²see <http://www.rri.res.in/DISTORTION/saras.html>

If the residual on fitting these spectra as the sum of a Planckian and MS function is at the level of a few mK, the foregrounds may be considered to be smooth at a level required to discern the EoR signal. This would provide impetus to use the MS function to separate foregrounds from the more complex cosmological signal. However, if the foreground spectra are themselves not smooth, the residuals in this exercise would be large, possibly larger than the EoR signal, which would indicate that there may potentially be spectral structure in the foregrounds that may limit or prohibit detection of the EoR signal, particularly if adopting signal extraction strategies that assume smooth foregrounds.

Inferences from the above exercise, whose results are presented in Fig. (9), are summarized below.

- When mock observations of sky spectra are generated from a physically-motivated sky model, and made with wide frequency-independent beams and over the entire LST range, MS functions are capable of accurately modeling the shape of the foreground component to leave residuals less than 5 mK, demonstrating that the foreground spectrum is indeed smooth to such precision. It follows that if the mock spectrum contains the generic EoR signal, which is inherently not smooth over the 40–200 MHz wide band, the residual on fitting such a spectrum with an MS function would be expected to be dominated by the EoR signal, with a smooth baseline subtracted. The smooth foreground would be largely removed and thus separated from the EoR signal. This expectation, which is based on the above analysis, is demonstrated below in Section 5.
- Spectra that have relatively lower contamination from the Galactic plane and Galactic center are fit by MS functions to greater absolute precision and yield residuals that have RMS of ~ 0.01 mK, which is substantially lower than the amplitude of the expected EoR signal. However, spectra at LSTs at which there is relatively large contribution from the Galactic plane and Galactic center yield residuals with RMS of up to 2–5 mK when fit with MS functions. As discussed in Sathyanarayana Rao et al. (2016), spectra towards the Galactic plane have more complex spectral shapes.

In Figure 10 is shown the RMS of residuals obtained on fitting MS functions to model foregrounds, versus the mean temperature of the corresponding spectrum. This is shown for the four sets of data corresponding to the two sites and two beams as described above. The mock spectra were synthesized at separations of one hour and distributed over the entire 24 hr in LST. Clearly there exists a correlation between the mean temperature of the spectrum and the RMS of the residual.

- In the case of spectral measurements that are made with beams well off the Galactic centre, with minimal contribution from the Galactic plane, the mean temperatures are low and the corresponding residuals have an RMS lower than 1 mK. We find that an eighth order MS function is sufficient to fit the foreground to a level that is lower than most predicted EoR signals. Therefore, provided observations are made at LSTs where Galactic contamination is relatively low, the foreground will be removed to relatively high precision. Towards these sky directions, any global EoR signal in a class of models similar to the vanilla model, with multiple inflections in the band, is expected to be detectable in the residual.
- On the other hand, for spectra toward regions of the sky that are intrinsically brighter, such as those towards the Galactic center, the RMS of the residual on fitting MS functions is higher. The highest RMS is expected for spectra recorded at MRO with a \cos^2 beam, when the Galactic centre transits nearly overhead. This is despite fitting with an MS function of order 10 and there is no significant change in the residual on increasing the order of the MS function to even 20. However, the RMS is at worst a few mK, which implies that even towards these directions that have significantly larger brightness,

generic models of the EoR signal can nevertheless be usefully distinguished from the foreground. On the other hand, since these regions do have relatively brighter emission with more complex spectral shapes, and the fitting process is computationally challenging, it is best to avoid the Galactic plane ($\pm 10^\circ$) and the Galactic centre while attempting to detect the weak global EoR cosmological signal.

For various large-area samplings of the sky, we have thus demonstrated that the foreground component in a beam-averaged spectrum is adequately describable by an MS function. Since even with arbitrarily large order for the MS function only smooth components are fitted out, foregrounds in spectra that are fit to mK levels by MS functions of any order are classified as smooth. Thus for observations with a frequency-independent beam, MS functions can be used to separate foregrounds from the global EoR signal. We next discuss mathematical statistical detection based on MS-form modeling of foregrounds.

5. On the detection of the global reionization signal

A sample spectrum representing a mock observation of the radio sky as observed by a \cos^2 beam is shown in Fig. (11). A GMOSS model for the sky has been adopted, and CMB with a spectral distortion corresponding to global EoR has been added in the making of the mock observation. We fit this mock observation of the sky spectrum with a function given by the sum of an MS function to describe the foreground and a Planck spectrum to account for the undistorted CMB, as described by Equation 6. We use the downhill simplex (Nelder & Mead 1965) optimization algorithm to iteratively fit this model to the synthetic spectrum adopting a successive approximation strategy. The MS polynomial is expressed as a Taylor expansion about a frequency given by the parameter p_1 . The first iteration fits a function that has four parameters: the CMB temperature p_0 , the Taylor expansion point p_1 and two coefficients that describe a single power law for the foreground. We successively include more terms using the optimized parameters from the previous iteration as initial guess and zero for the new coefficient introduced. The residuals on subtracting a model with a Planckian function and MS functions of degree 2, 5, 7, 8, 10 and 15 are also shown in Fig. (11). This may be compared to the residuals obtained above on fitting unconstrained polynomials to a mock observation containing the EoR signal, which was shown in Fig. (6). As noted earlier, for the case where the foregrounds were modeled as unconstrained polynomials the residual amplitude gets progressively lower with increasing polynomial order and there are additional turning points introduced. On the other hand, while using MS functions, the residual remains unchanged once the MS function encounters a shape that cannot be described as smooth and thenceforth increasing the order of the MS function no longer changes the residual. This would continue to be the case on fitting the spectrum with MS functions of arbitrarily higher order. The residual recovered on fitting the mock spectrum with such components that may accurately model the CMB and foreground appears qualitatively similar to the adopted global EoR signal, which was included in the simulation. We now proceed to quantify the confidence in signal detection and the likelihood of false positives.

We adopt a Bayes Factor (BF) approach to quantify signal detection as described in Sathyanarayana Rao et al. (2015). The Bayes Factor is the Bayesian equivalent of the Maximum likelihood of detection in frequentist statistics. Given a dataset D , BF gives the more probable of two models M_1 and M_2 with parameters θ_1 and θ_2 respectively. BF is expressed as

$$BF = \frac{P(D|M_1)}{P(D|M_2)} = \frac{\int P(\theta_1|M_1)P(D|\theta_1, M_1)d\theta_1}{\int P(\theta_2|M_2)P(D|\theta_2, M_2)d\theta_2}. \quad (7)$$

For the case where both the models are equally likely, the ratio of priors is unity. This is assumed here:

that it is as likely that an EoR model is present in an observation as not, and all plausible EoR models are *a priori* equally likely. If the outcome of the test is that model M_1 is more likely than M_2 , then the BF is expected to be large (greater than unity) and if M_2 describes the data better than M_1 , then BF is expected to be small (less than unity).

The likelihood for any model M is given by:

$$P(D|M) = \prod_{i=1}^N \frac{e^{-\frac{y_{res}[i]^2}{2\sigma^2}}}{\sqrt{2\pi\sigma^2}}, \quad (8)$$

where N is the number of independent points across the spectrum and $y_{res}[i]$ is the residual spectrum following subtraction of the corresponding model from the data D . The variance of the measurement noise, σ^2 , is assumed to be half the Allan Variance of the residual and is estimated from the data using the relation:

$$\sigma^2 = \frac{1}{2} \sum_{i=1}^{N-1} (y_{res}[i+1] - y_{res}[i])^2. \quad (9)$$

In this work, for the purpose of demonstrating the value of MS function approach to modeling the foreground, we consider only the vanilla model for global EoR and use the BF test to compare between two models $M1$ and $M2$ that correspond, respectively, to a function describing foreground plus CMB plus EoR and a second function that models only the foreground and CMB:

$$M1: T(\nu) = \left(\frac{h\nu}{k}\right) / \left(e^{\frac{h\nu}{kp_0}} - 1\right) + 10^{\sum_{i=0}^N [\log_{10}(\nu/p_1)]^i p_{i+2}} + y_t(\nu) \quad (10)$$

and

$$M2: T(\nu) = \left(\frac{h\nu}{k}\right) / \left(e^{\frac{h\nu}{kp_0}} - 1\right) + 10^{\sum_{i=0}^N [\log_{10}(\nu/p_1)]^i p_{i+2}}. \quad (11)$$

Here $y_t(\nu)$ is the template of the EoR signal at frequency ν and the remaining terms are the same as in Equation 6.

Consider two mock spectra that might separately represent the dataset D , one that contains the EoR signal and the other that does not. For the two models $M1$ and $M2$ defined above, we would expect the BF for the spectrum that contains the EoR signal to be larger than unity and that for the spectrum that does not contain the signal to be less than unity. However, this may not necessarily be the case in the presence of noise. For large noise and poor signal to noise ratio, it is statistically possible that the particular mock spectrum that does not contain EoR erroneously yields a large value for BF. This would lead to a mistaken conclusion that the EoR signal is indeed present in the data when there is none, thus giving a false positive detection. On the other hand, it is also statistically possible for the spectrum containing the EoR to yield a small BF leading to the erroneous interpretation that the signal is not present in the measurement. Both such incorrect inferences are best avoided by observing for sufficient time and attaining adequate sensitivity. An examination of the distribution of BFs for varying amounts of noise, or equivalently the integration time, can guide the interpretation of the BF by assigning appropriate confidence to outcomes of experiments.

We generate two data sets ‘a’ and ‘b’ of 100 mock spectra each. While spectra in dataset ‘a’ contain the vanilla model of the EoR signal added to them, spectra in dataset ‘b’ do not. We also introduce Gaussian random noise in spectra of both datasets. The noise corresponds to that in a correlation spectrometer

measuring a difference spectrum between the antenna temperature and reference load; we assume a scheme similar to that adopted in Patra et al. (2015). The variance ΔT of the added Gaussian noise is given by

$$\Delta T = \sqrt{\frac{[(5/4)(T_a + T_{\text{ref}})^2 + (T_a + T_{\text{ref}})(T_{n1} + T_{n2}) + T_{n1}T_{n2}]}{2\Delta\nu\Delta t}}. \quad (12)$$

Here, T_a is the antenna temperature, T_{ref} is the temperature of a reference load that serves to provide a baseline against which the antenna temperature is measured, T_{n1} and T_{n2} give the effective amplifier noise temperatures in the two paths of the receiver that feed into the correlation spectrometer. We assume values $T_{\text{ref}} = 300$ K, $T_{n1} = T_{n2} = 50$ K. T_a in each channel of bandwidth $\Delta\nu = 1$ MHz is given by the noise-free antenna temperature of the mock spectrum in the corresponding channel. Spectra with varying amounts of noise are generated by varying the integration time Δt .

For every spectrum from each of the two data sets we obtained two residuals by fitting models $M1$ and $M2$ given by Equations 10 and 11 respectively. The corresponding likelihoods are computed using Equation 8 and these are then used to compute the BF for the said spectrum using Equation 7. Thus, from the spectra of the two data sets, we obtain two distributions of BFs for any particular noise variance. If the two BF distributions are disjoint and have no overlap, the computed BF would be an indicator of the presence or absence of the EoR signal in the measurement. However, if the distributions have significant overlap, then a result that is a BF from the overlap domain would be uncertain and results that are outside this overlap domain would be more conclusive. If the detection strategy is a useful one, the BF distributions would be expected to be increasingly disjoint for decreasing noise and thus increasing integration time.

The distributions in BFs for the pair of data sets were computed for three different integration times. In Fig. (12a) we show these distributions for detection with 75% confidence and delineate the divergence in the distributions with increasing integration time. The median values of the distributions are marked using filled circles about which the distribution is presented as a red shaded region for spectra from data set ‘a’ and as green shaded region for spectra from data set ‘b’. In order to represent regions with 75% confidence in this Panel (a), the width of the distribution is chosen to be the region in which 75% of the BF samples lie. For greater confidence in any detection, we include a correspondingly greater fraction of samples in the delineated regions, and the regions would diverge at correspondingly greater integration times. For example, Fig. (12b) is for detection with 95% confidence. Since increasing the MS function to arbitrarily high orders does not change the residuals, as demonstrated by Fig. (7b), increasing the order of the MS function does not change the results presented in Fig. (12).

The above approach that uses MS functions to model the foreground and BFs to arrive at an interpretation may be compared with the equivalent BF distribution plots for the case where the foreground component in the models $M1$ and $M2$ are described using unconstrained polynomials instead of MS functions. The order of the polynomials is fixed to be seven; as discussed in Section 3.3, this is the necessary and sufficient order for polynomials to fit foregrounds that are generated using a GMOSS sky model. The resulting BF distributions for 95% confidence when using polynomials of order 7 and 20 are shown in Fig. (13).

In both cases the distributions of BFs for data sets with and without the EoR signal diverge at integration times larger than those for the case when using MS functions. Firstly, fitting data with such polynomials degrades the SNR by fitting out a substantial part of the EoR signal itself along with the foreground. The functional form of the foreground spectrum is a priori unknown and using a polynomial of arbitrary order degrades the SNR. This downside is all the more severe when polynomials of high orders are adopted to describe the foreground. Clearly, the integration time required to distinguish between the presence or absence of the generic EoR signal using a Bayes Factor test is larger when a polynomial of order 20 is used

compared to the case when a polynomial of order 7 is used, which is in turn larger than the case when MS functions are used. Second, residuals of such fits with high-order polynomials may well mimic plausible EoR signal shapes, hence leading to degeneracy between the EoR signal and residuals produced on fitting spectra with polynomials. Thus the ability to distinguish between the presence or absence of the EoR signal is compromised by modeling the foregrounds as polynomials of high order as opposed to the more robust method of using MS functions to model foregrounds.

If we assume that we use the BF method to detect the presence of the vanilla model of global EoR, and compare the two hypotheses corresponding to the presence of the vanilla model versus absence of any EoR signature, we may examine the confidence level at which the BF distributions diverge versus integration time. The resulting curve is shown as a solid line in Fig. (14). We see that using a BF test with MS functions to model foregrounds, it is possible to detect the presence of the EoR signal with 95% confidence in 10 minutes effective integration time using a correlation spectrometer with system parameters as described above. It may be noted here that this result is for models that are similar in nature to the vanilla model of the EoR signal, which has multiple turning points in the frequency range of 40–200 MHz, and has a shape that is distinct and distinguishable from smooth foregrounds using MS functions.

For the corresponding case of modeling of foregrounds using polynomials of order 7 and 20, the confidence in detection of signals and in rejection of false positives are given as a dashed-dot line and dashed line respectively in Fig. (14). We see that if a BF test is done using a polynomial of order 7, an effective integration time of at least 18 minutes is required to detect the presence of the EoR signal with 95% confidence, which is double the time required when using MS functions. This number increases to 72 minutes when using a polynomial of order 20. Thus, choosing a polynomial of different orders can result in different confidence in detection for the same integration time with the same instrument. The interpretation as signifying either the presence or absence of the EoR signal in a measurement set can critically depend on the order of the polynomials used to describe foregrounds or system parameters, unless supported by other methods to quantify signal detection. Additionally and more importantly, MS functions are robust in that even with increasing order they do not subsume EoR models with inflections; therefore, it is preferable to use MS functions to model foregrounds and distinguish the cosmological 21-cm signal.

6. Conclusions and Summary

Towards detection of the global redshifted 21-cm signal from reionization, we have done simulations of spectral radiometer observations in the 40–200 MHz band with widefield antennas. The specific aim has been to study the spectral shapes expected for the foreground, whether these might confuse or limit detection of the expected wideband cosmological signatures, and examining methods for their modeling. This work is an improvement over previous studies in that we have adopted a physically motivated sky model GMOSS and examined the efficacy of modeling the foreground as *Maximally Smooth* functions. The new approach to global EoR detection has been compared with previous modeling of foregrounds as polynomials in $\log(T)$ vs $\log(\nu)$ space. Mock data corresponding to contrasting beam shapes, site latitudes and the full range of observing sidereal times have been considered.

The work leads to the conclusion that wideband wide-field sky spectra as measured by radiometers attached to frequency independent antennas are expected to be Maximally Smooth to the precision necessary for detection of vanilla or generic predictions for the global EoR signal. We have demonstrated that modeling foregrounds using Maximally Smooth functions is advantageous for the detection of global Epoch

of Reionization signals that have multiple turning points in the observing frequency band. The MS function can selectively fit to any smooth foreground and CMB with arbitrary precision by allowing for a sufficiently large order for the fitting function, and despite the high order such a modeling would leave a residual that contains most of the global EoR signal. Most importantly, the residual following MS function fitting preserves turning points that define the critical epochs in the cosmological evolution of the baryons during the Dark Ages, First Light or Cosmic Dawn and reionization.

The MS function approach to modeling the foreground has been demonstrated to be amenable to a successive approximation type of solution for the model parameters. The MS function coefficients may be expanded as a Taylor series and solved for iteratively by increasing the polynomial order successively while progressively approximating the foreground with greater accuracy. There is no loss of signal in the residual if the order of the MS function were increased arbitrarily and hence the approximation may be continued to degrees well beyond what is needed and until the higher order fitting coefficients are found to be negligible. The amplitude of the EoR features is thus largely recovered and, unlike in the case of the hitherto adopted polynomial fitting approach, the amplitude is undiminished with increasing order of the fitting function.

The MS-function modeling approach suggested herein may be viewed as a filter that progressively, and in successive approximations, removes or filters out the smooth component of the data while leaving behind the non-smooth component, for increasing orders of the MS function. After having filtered out all the smooth components of the signal, further increasing the order of the MS function no longer affects the residual, resulting in a ‘saturated residual’.

The invariance of the residual when fitting with MS functions with higher orders than needed to represent the foreground, and the success in accurately modeling the foregrounds for mock observations corresponding to different sky directions, site latitudes, telescope beam types and observing LSTs demonstrates the robustness of the MS function approach as opposed to simple polynomial fits.

Our work that uses the physically-motivated GMOSS sky model suggests that the foreground is indeed Maximally Smooth to the required precision for detection of global EoR. Nevertheless, we conclude by briefly discussing the consequence of non-smooth foreground components, which may manifest as spurious residuals following MS modeling of spectral data, particularly in observations made towards the Galactic Center and plane. If the foreground spectrum is itself not smooth at a level above the EoR signal, fitting the sky spectrum with an MS function will fail to fit the non-smooth part of the foreground, and the EoR signal will appear confused in this foreground residual. This consideration leads to the question that if an observation of the sky spectrum is fit with an MS function of a high order, and if the residual is not diminished any further by increasing the order of the MS function, then how do we distinguish between residuals that are EoR signals from any non-smooth foreground? A solution to this problem may be found in joint analysis of sky spectra observed separated in LST so that they contain different samplings of the sky, and hence different foreground spectra. Saturated residuals that differ between different regions of the sky is indicative of spectral structure in foreground spectra and a changing residual may be used to “dissever foreground components” and hence separate this non-smooth part of the foreground from global EoR (Switzer & Liu 2014). However, if the saturated residuals towards different regions of the sky after fitting with MS functions of arbitrarily high order are the same in structure and amplitude, it would be highly suggestive that the residual is global in nature, making a case for EoR signal detection. Comparing the residual with smooth baseline subtracted templates, which may be obtained by subtracting MS functions from predictions for global EoR signals in various models, would provide the ability to distinguish between EoR scenarios.

We have presented a Bayes Factor approach to estimate the integration time necessary to detect with

varying levels of confidence the presence or absence of global EoR signal in sky spectra, when MS functions are used to model the foreground. We have also compared with the case where polynomials are used to model the foreground. We have found that a fit to recorded sky spectra using an MS function provides the advantage of signal detection with improved signal-to-noise ratio as compared to the polynomial case. A receiver noise temperature of ~ 50 K, as has been assumed in our analysis above, is achievable. However, making a frequency independent antenna over multi-octave bandwidths is non-trivial. Nevertheless, with such a well designed antenna and spectral radiometer, our analysis indicates that with about 1000 sec effective integration the global EoR signal may be detected with 95% confidence using MS functions.

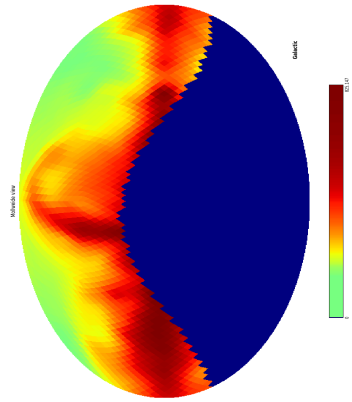
7. Acknowledgements

JC is supported by the Royal Society as a Royal Society University Research Fellow at the University of Cambridge, U.K.

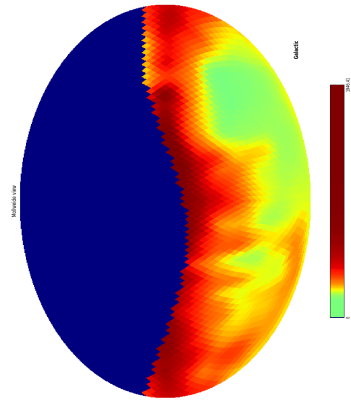
REFERENCES

- Ali-Haïmoud, Y., & Hirata, C. M. 2011, *Phys. Rev. D*, 83, 043513
- Bernardi, G., McQuinn, M., & Greenhill, L. J. 2015, *ApJ*, 799, 90
- Calabrese, E., Hlozek, R. A., Battaglia, N., et al. 2013, *Phys. Rev. D*, 87, 103012
- Chluba, J., & Thomas, R. M. 2011, *MNRAS*, 412, 748
- de Oliveira-Costa, A., Tegmark, M., Gaensler, B. M., et al. 2008, *MNRAS*, 388, 247
- Farhang, M., Bond, J. R., Chluba, J., & Switzer, E. R. 2013, *ApJ*, 764, 137
- Field, G. B. 1958, *Proceedings of the IRE*, 46, 240
- Furlanetto, S. R., Oh, S. P., & Briggs, F. H. 2006, *Phys. Rep.*, 433, 181
- Glover, S. C. O., Chluba, J., Furlanetto, S. R., Pritchard, J. R., & Savin, D. W. 2014, *Advances in Atomic Molecular and Optical Physics*, 63, 135
- Gnedin, N. Y., & Shaver, P. A. 2004, *ApJ*, 608, 611
- Górski, K. M., Hivon, E., Banday, A. J., et al. 2005, *ApJ*, 622, 759
- Harker, G. J. A. 2015, *MNRAS*, 449, L21
- Haslam, C. G. T., Salter, C. J., Stoffel, H., & Wilson, W. E. 1982, *A&AS*, 47, 1
- Landecker, T. L., & Wielebinski, R. 1970, *Australian Journal of Physics Astrophysical Supplement*, 16, 1
- Mozdzen, T. J., Bowman, J. D., Monsalve, R. A., & Rogers, A. E. E. 2016, *MNRAS*, 455, 3890
- Nelder, J. A., & Mead, R. 1965, *The Computer Journal*, 7, 308
- Patra, N., Subrahmanyan, R., Sethi, S., Udaya Shankar, N., & Raghunathan, A. 2015, *ApJ*, 801, 138
- Planck Collaboration, Adam, R., Ade, P. A. R., et al. 2016a, *A&A*, 594, A1
- Planck Collaboration, Adam, R., Aghanim, N., et al. 2016b, *ArXiv e-prints*, arXiv:1605.03507
- Pritchard, J. R., & Loeb, A. 2010, *Phys. Rev. D*, 82, 023006
- Raghunathan, A., Shankar, N. U., & Subrahmanyan, R. 2013, *IEEE Transactions on Antennas and Propagation*, 61, 3411
- Reich, P., & Reich, W. 1986, *A&AS*, 63, 205
- Reich, W. 1982, *A&AS*, 48, 219

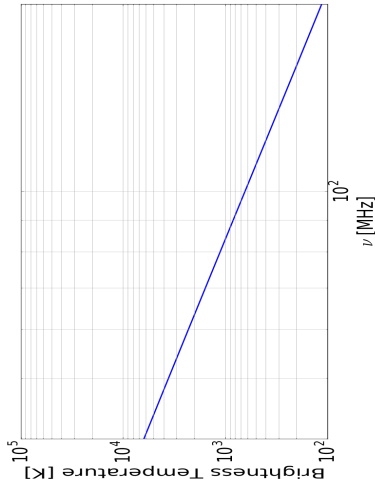
- Sathyannarayana Rao, M., Subrahmanyam, R., Udaya Shankar, N., & Chluba, J. 2015, ApJ, 810, 3
- Sokolowski, M., Tremblay, S. E., Wayth, R. B., et al. 2015, PASA, 32, e004
- Switzer, E. R., & Liu, A. 2014, ApJ, 793, 102
- Voytek, T. C., Natarajan, A., Jáuregui García, J. M., Peterson, J. B., & López-Cruz, O. 2014, ApJ, 782, L9
- Wouthuysen, S. A. 1952, AJ, 57, 31



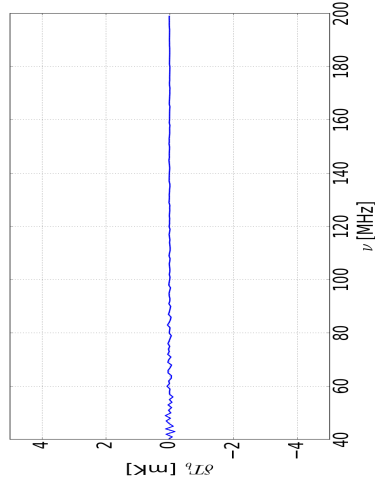
(a) \cos^2 beam Hamle



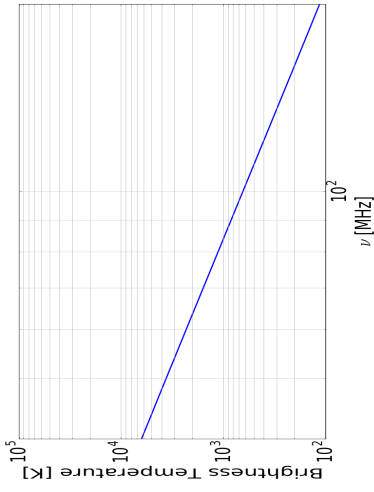
(b) \cos^2 beam MRO



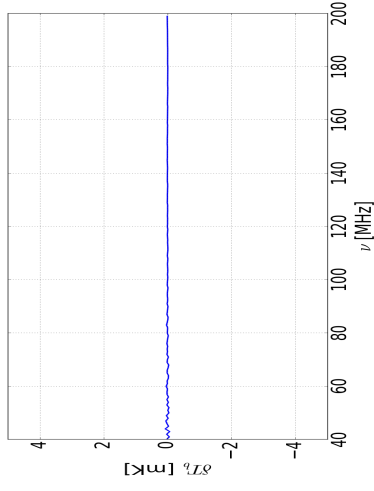
(c) Spectrum off Galactic Plane



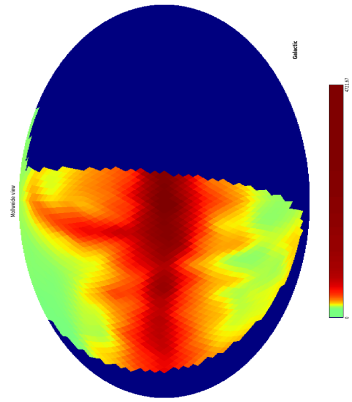
(e) Residual



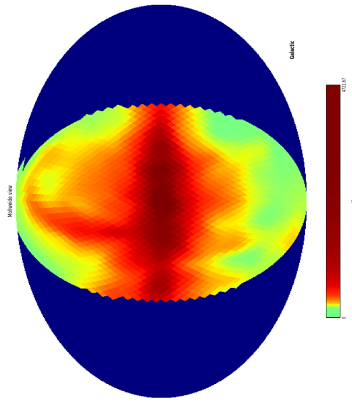
(d) Spectrum off Galactic Plane



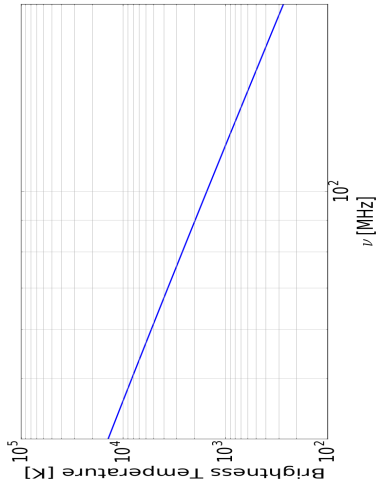
(f) Residual



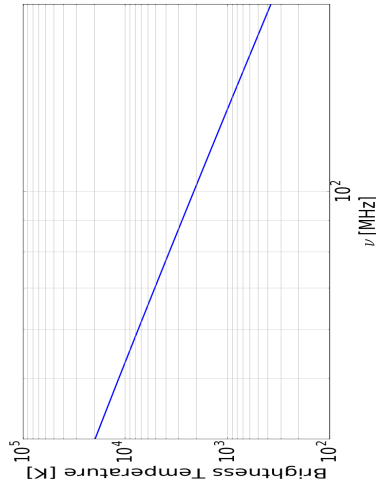
(a) \cos^2 beam Hanle



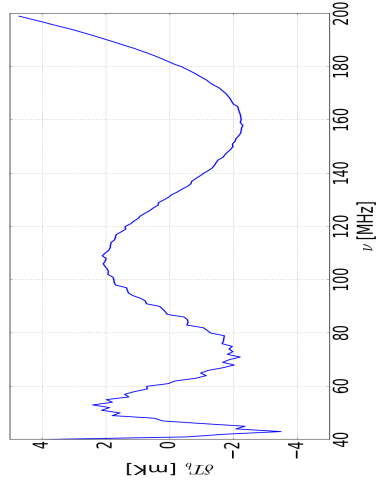
(b) \cos^2 beam MRO



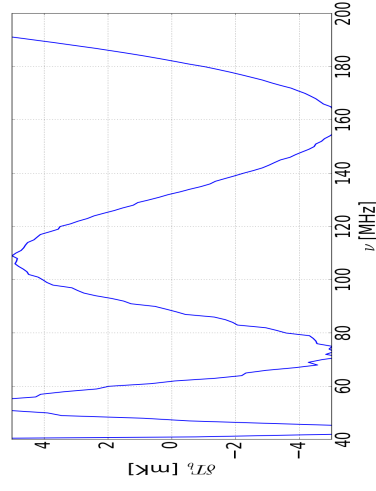
(c) Spectrum toward Galactic Plane



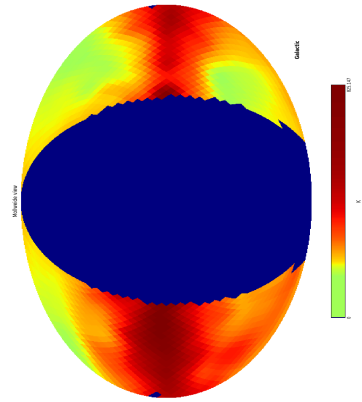
(d) Spectrum toward Galactic Plane



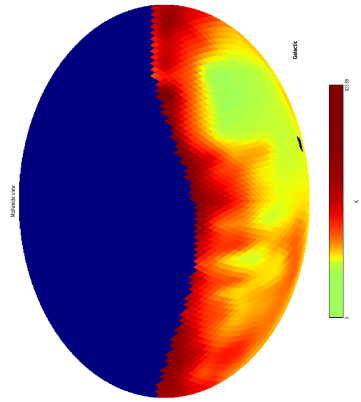
(e) Residual



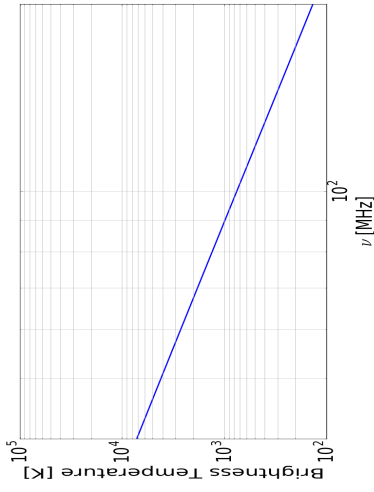
(f) Residual



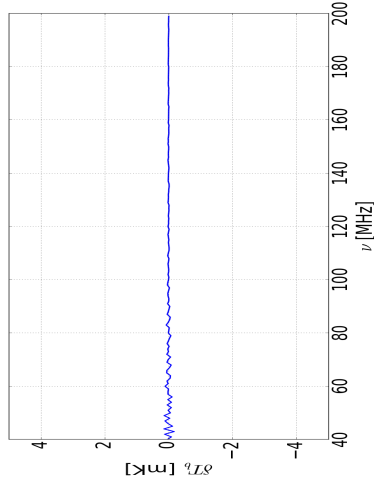
(a) SARAS2 beam Hanle



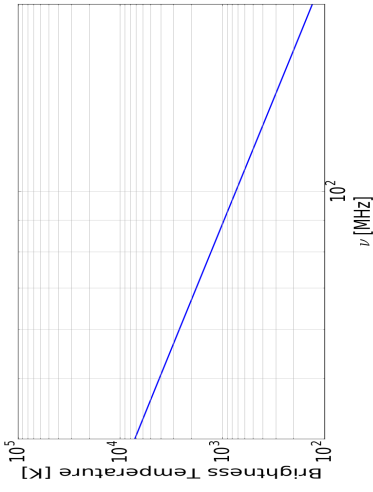
(b) SARAS2 beam MRO



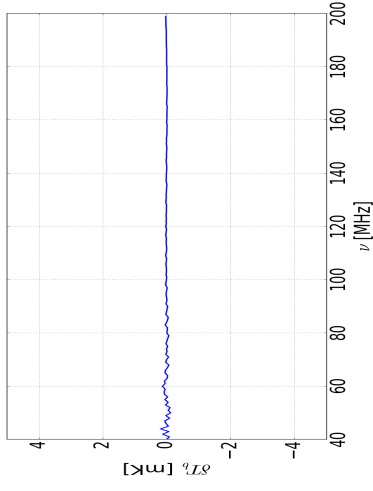
(c) Spectrum off Galactic plane



(e) Residual



(d) Spectrum off Galactic plane



(f) Residual

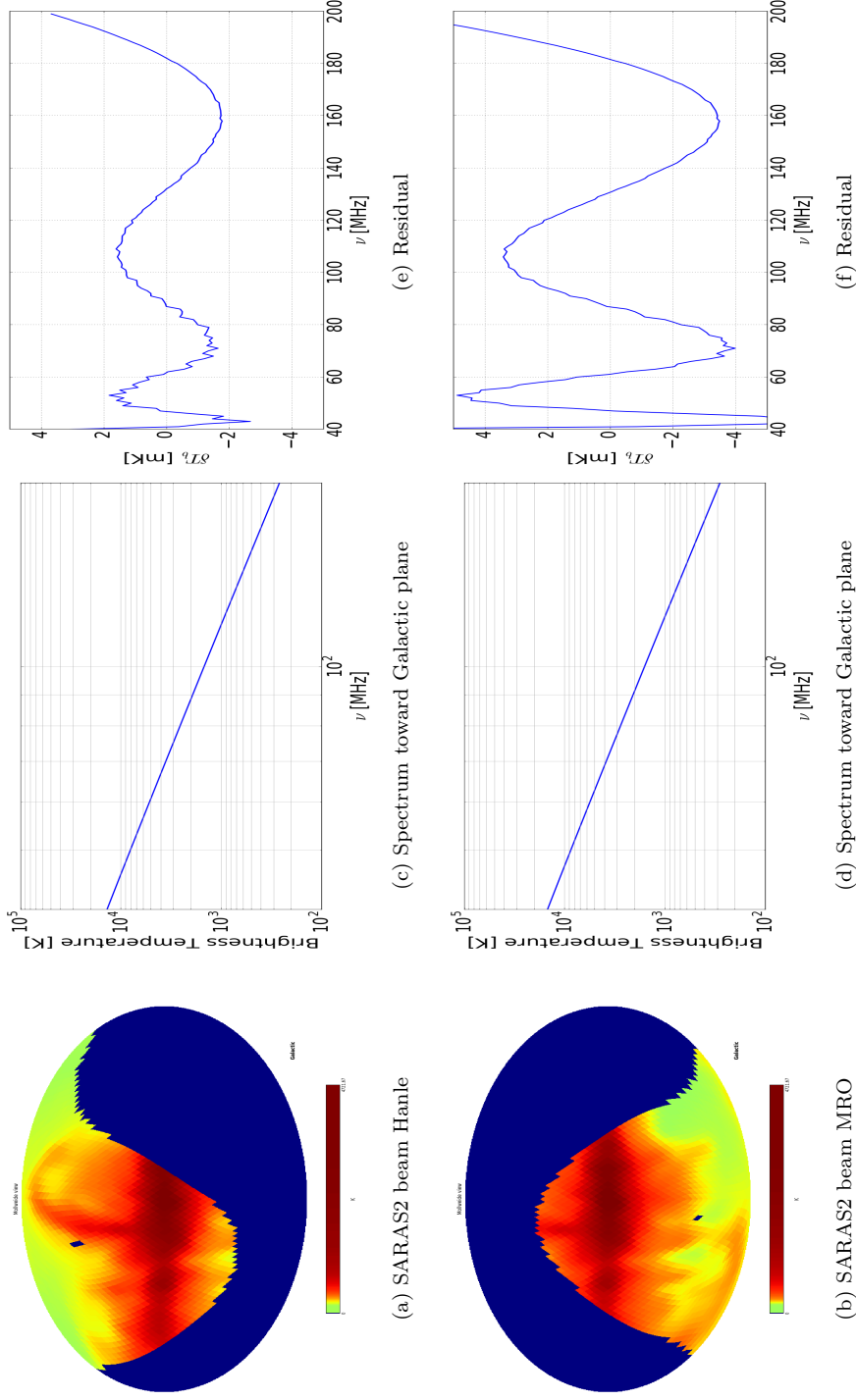
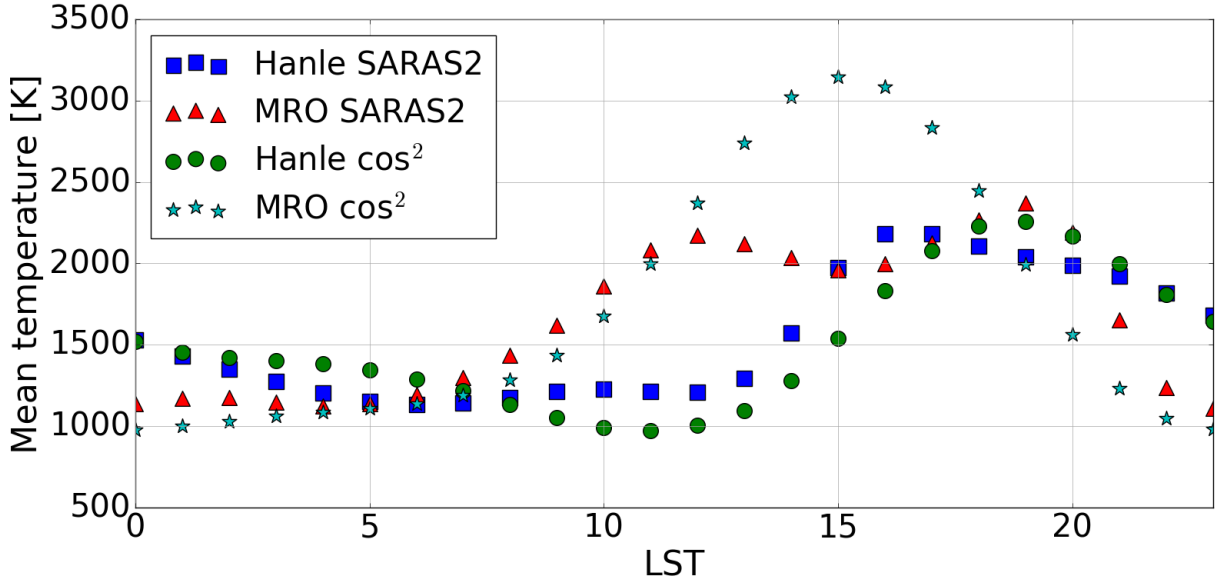
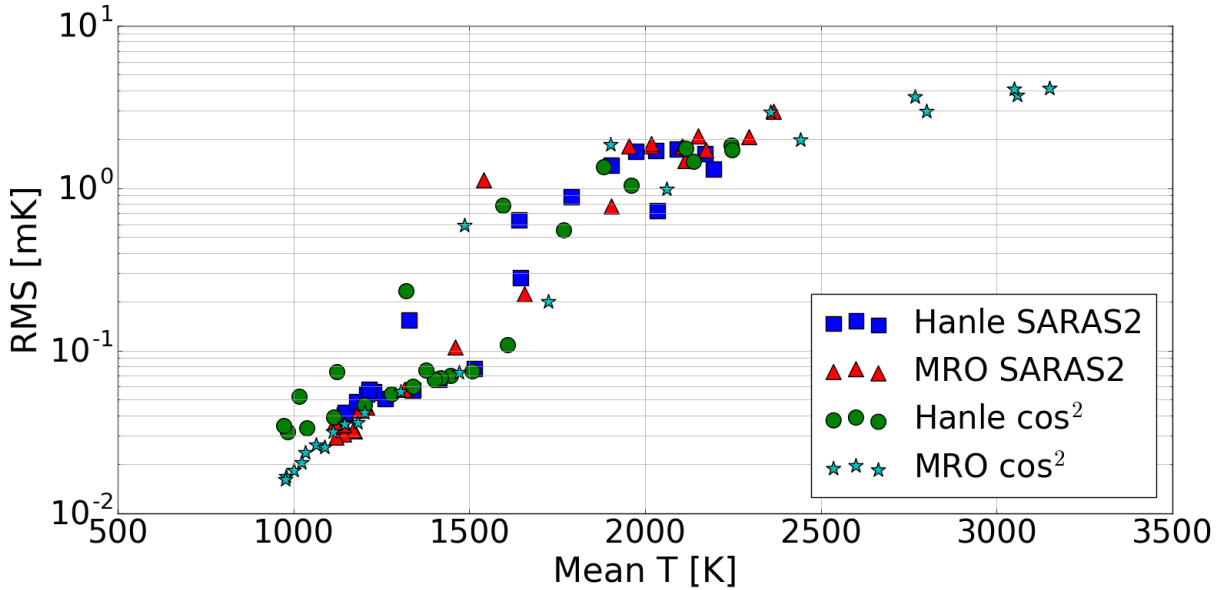


Fig. 9.— Testing the smoothness of foregrounds in mock sky spectra that are simulated using GMOSS as the sky model for two observing sites, namely Hanle (Latitude = 32.79°N) and MRO (Latitude = 26.68°S). The first column shows the pixels that lie in the antenna beam used to generate spectra; these are displayed on an all-sky map at 150 MHz with a resolution of 5° . Pixels that lie outside the beam are blanked. The spectra themselves are shown in the second column. The third column shows the residual on fitting these spectra with the form given by Equation 6. Spectra are simulated for two frequency-independent antenna beams, namely a \cos^2 beam and beam of the SARAS 2 short monopole antenna. In each of the observing sites considered, the spectra at the LSTs in which they have maximum and minimum foreground brightness are shown, as examples.



(a)



(b)

Fig. 10.— The mean temperature of mock spectra versus LST is shown in Panel (a). The RMS of residuals on fitting MS functions to these spectra is shown in Panel (b). The RMS residuals for spectra simulating observations with a \cos^2 beam at Hanle and MRO are shown as filled circles and filled stars respectively. The RMS of residuals for spectra simulating observations with the beam of the SARAS 2 antenna, at Hanle and MRO, are given by filled squares and crosses respectively. Clearly, the RMS residuals are larger for spectra that are brighter, which are those having relatively greater contribution from the Galactic plane. A spectrum recorded at MRO by an antenna with \cos^2 beam would have a maximum temperature at the LST when the Galactic center has the minimum zenith angle. This also corresponds to the spectrum having the largest RMS residual amongst the various mock spectra considered here.

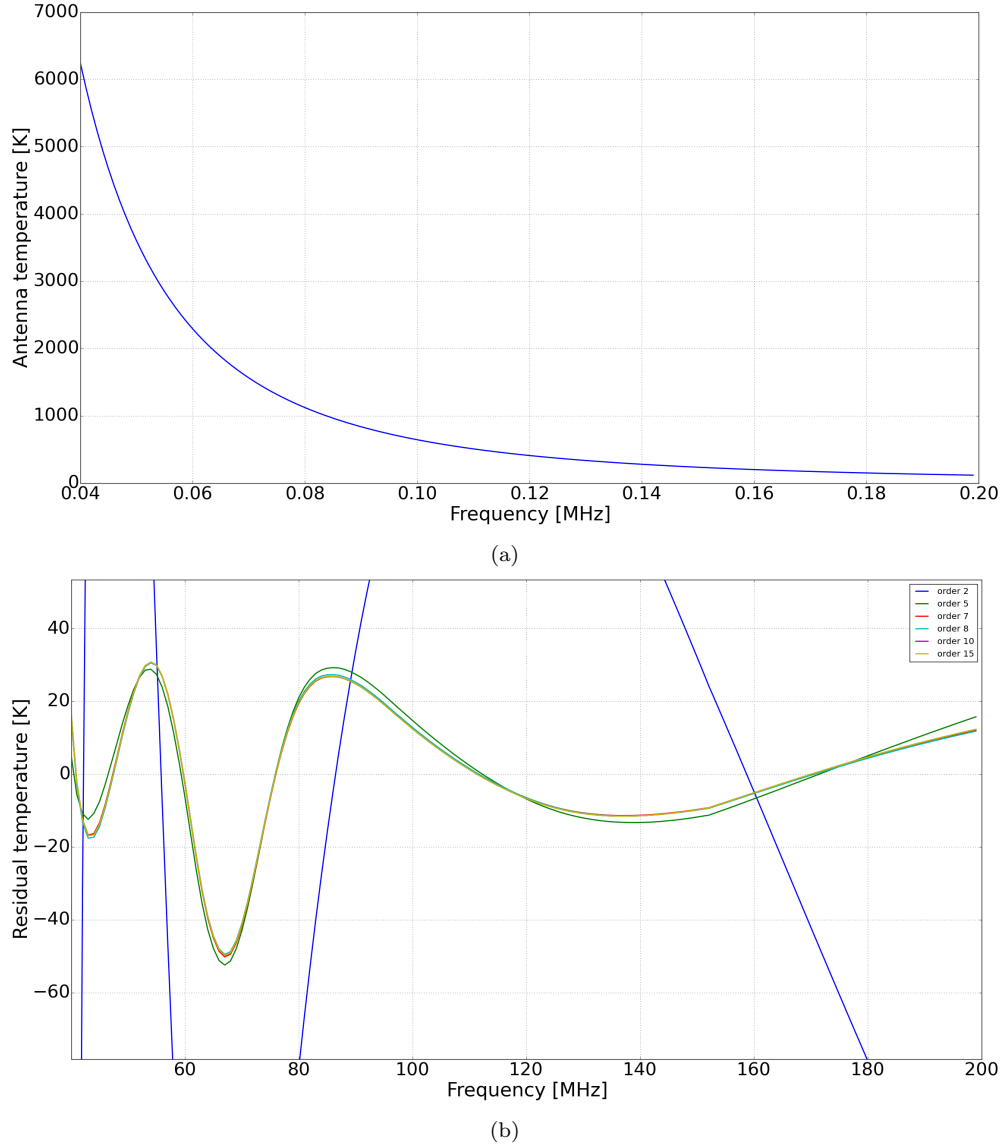
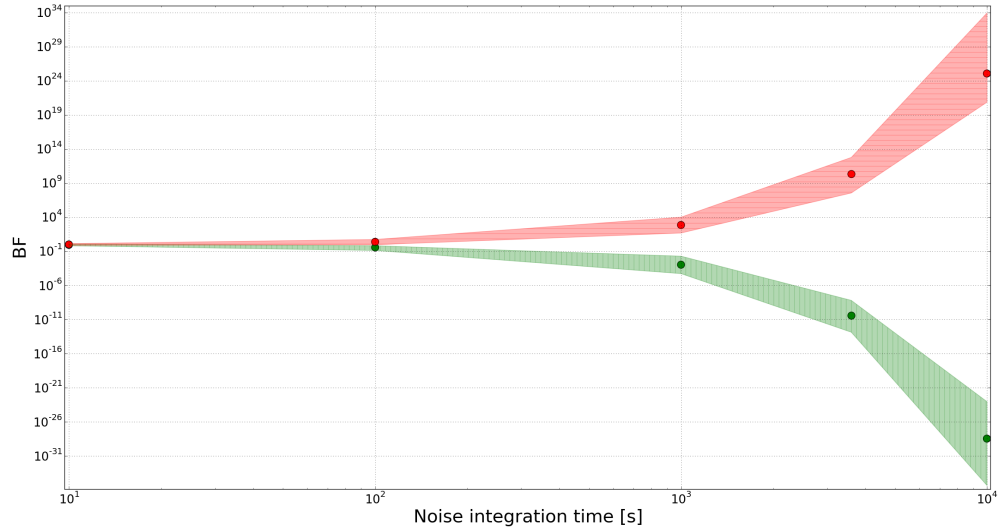
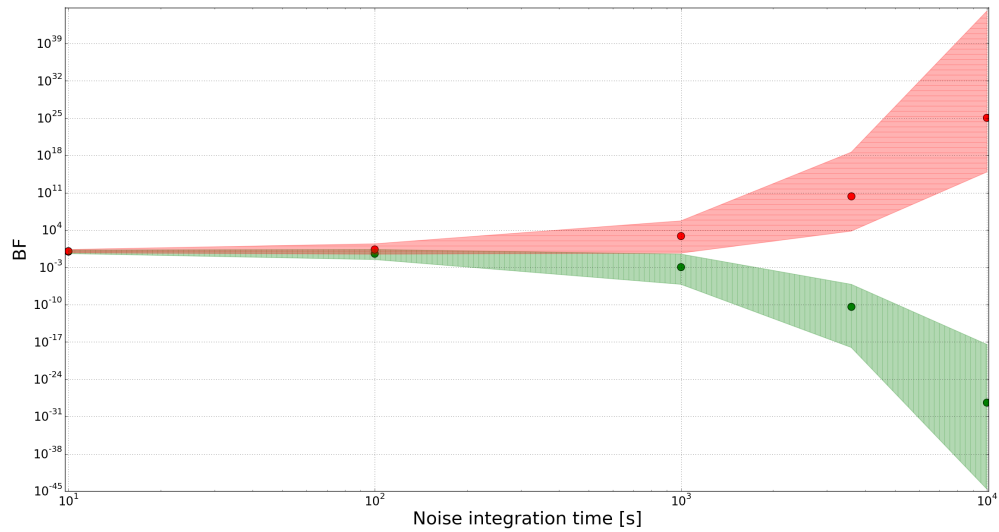


Fig. 11.— (a) A mock spectrum generated on observing the GMOSS sky with a frequency-independent \cos^2 beam. The spectrum also contains CMB with a distortion given by the vanilla model of the global EoR signal. (b) Residuals obtained on fitting the spectrum in Panel (a) with a Planck function plus separately MS functions of degree 2, 5, 7, 8, 10 and 15. Once the MS function has fit out all the smooth components in the spectrum, the residual no longer changes on increasing the order of the MS function. The residual essentially retains a large part of the EoR signal, with all turning points preserved.



(a) 75% confidence



(b) 95% confidence

Fig. 12.— The distribution of Bayes Factors versus integration time for spectra containing the EoR signal (red shaded region) and spectra without the EoR signal (green shaded region). The median Bayes factors are shown using filled circles. The point at which the two shaded regions diverge represents the integration time required to distinguish between the presence and absence of the signal in a measurement with a certain confidence. The confidence is given by the width of the shaded regions about the median value. For detection with greater confidence the regions diverge later, *i.e.*, at greater integration times. It may be noted that the models used to describe the spectra for BF estimation employ MS functions of order 8 to fit the foreground component.

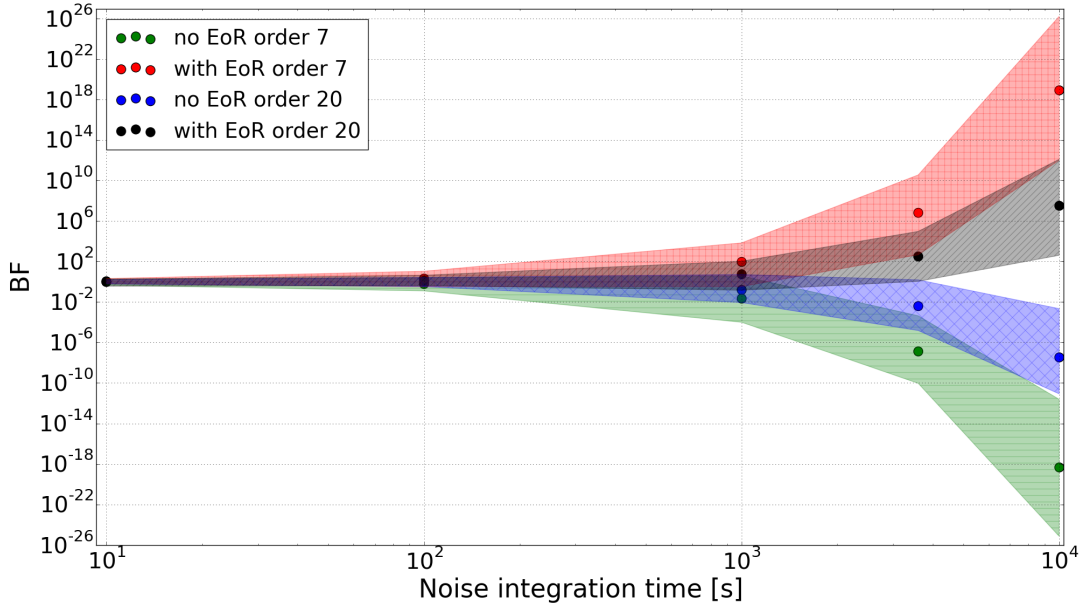


Fig. 13.— The distribution of Bayes Factors versus integration time for spectra containing the EoR signal and spectra without the EoR signal. The median Bayes factors are shown using filled circles. The point at which the two shaded regions diverge represents the integration time required to distinguish between the presence and absence of the signal in a measurement with 95% confidence. The red and green shaded regions represent Bayes Factor distributions on using a polynomial of order 7 to describe foregrounds. The black and blue regions denote Bayes Factors using a polynomial of order 20 to describe foregrounds. As expected, increasing the order of polynomial results in the two sets of Bayes Factors (with and without the EoR signal) diverging at larger integration times. This is because the signal-to-noise ratio degrades as more of the signal is erroneously subsumed in the foreground as the order of the fitting polynomial is increased.

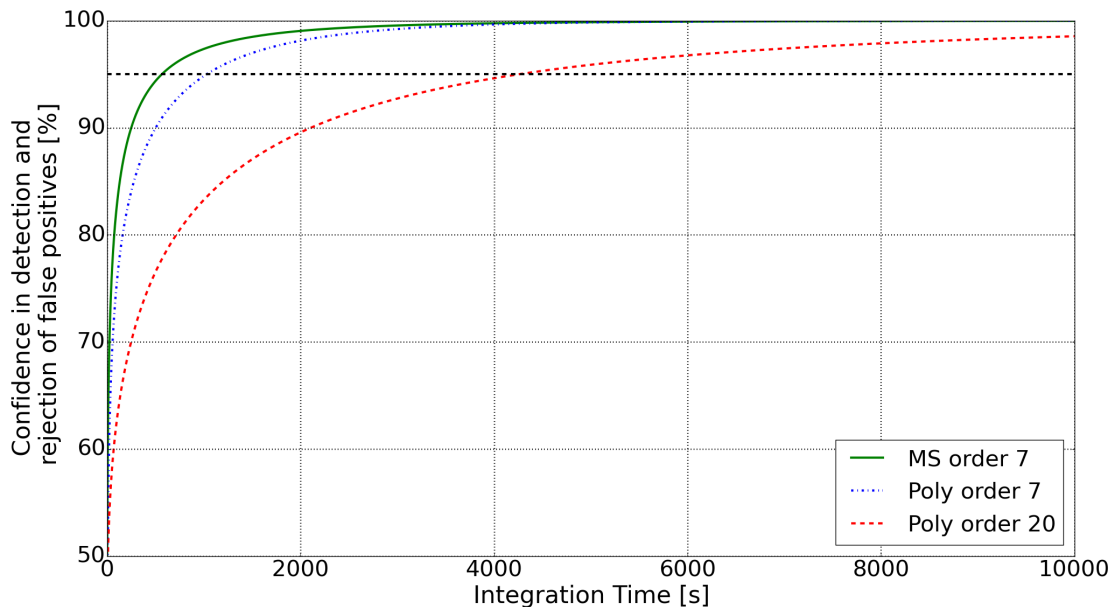


Fig. 14.— The confidence in detection of a signal using the BF test versus integration time. The BF test that employs models that use the MS function to fit to the foreground component in spectra is shown as a solid green line. For noise as given by Equation (5), corresponding to a correlation spectrometer scheme described in Patra et al. (2015), an effective integration time of 0.16 hours or 10 minutes results in 95% confidence detection of the vanilla model global EoR signal, along with rejection of false positives with same confidence. Also shown are confidence in detection using BF test for models that use polynomials of order 7 (blue dashed-dot line) and order 20 (dashed red line) to model the foreground component in spectra. As seen from the figure, increasing the order of the polynomial used results in that a larger integration time is required to reach the same level of confidence; we interpret this as due to the degradation in signal to noise ratio as more of the global EoR signal is subsumed in the foreground model. For a polynomial of order 7 an integration time of 18 minutes results in 95% confidence detection and also confidence in rejection of false positives. For the case of an order 20 polynomial this increases to 72 minutes. In both cases the integration time required is larger than when using MS functions to model the foreground.